Article

Not peer-reviewed version

Impact of Epstein-Barr Virus Nuclear Antigen 1 on Neuroinflammation in PARK2 Knockout Mice with Mitochondrial Dysfunction

Davide Cossu *, Yuji Tomizawa, Sachiko Noda, Eiichi Momotani, Tamami Sakanishi, Hanna Okada, Kazumasa Yokoyama, Leonardo A. Sechi, Nobutaka Hattori

Posted Date: 26 August 2024

doi: 10.20944/preprints202408.1776.v1

Keywords: Epstein-Barr Virus; PARK2 Knockout Mice: Mitochondrial Dysfunction

 doi:10.20944/preprints202408.1776.v1

Article

Impact of Epstein-Barr Virus Nuclear Antigen 1 on Neuroinflammation in PARK2 Knockout Mice with Mitochondrial Dysfunction

Davide Cossu [1,2,3,*], Yuji Tomizawa [1], Sachiko Noda [1], Eiichi Momotani [4], Tamami Sakanishi [5], Hanna Okada [1], Kazumasa Yokoyama [1], Leonardo Antonio Sechi [3,6] and Nobutaka Hattori [1,7]

[1] Juntendo University, Department of Neurology, 1138431 Tokyo, Japan
[2] Juntendo University, Biomedical Research Core Facilities, 1138431 Tokyo, Japan
[3] Sassari University, Department of Biomedical Sciences, 07100 Sassari, Italy
[4] Comparative Medical Research Institute, Tsukuba 305-0856, Japan
[5] Juntendo University, Division of Cell Biology, 1138431 Tokyo, Japan
[6] Struttura Complessa di Microbiologia e Virologia, Azienda Ospedaliera Universitaria, 07100 Sassari, Italy
[7] Neurodegenerative Disorders Collaborative laboratory, RIKEN Center for Brain Science, 3510918 Saitama, Japan
* Correspondence: D.C. davide@juntendo.ac.jp

Abstract: This study aimed to explore the intricate relationship between mitochondrial dysfunction, infections, and neuroinflammation, focusing specifically on the impact of pathogenic epitopes of *Epstein-Barr Virus* (EBV) nuclear antigen 1 (EBNA1) in a mouse model of mitochondrial dysfunctions. The investigation included female middle-aged *PARK2*$^{-/-}$ and C57BL/6J wild-type mice immunized with EBNA1$_{386-405}$ or with active experimental autoimmune encephalomyelitis (EAE) induction by myelin oligodendrocyte glycoprotein (MOG)$_{35-55}$ peptide. *PARK2*$^{-/-}$ mice developed more severe EAE than wild-type mice. Following immunization with EBNA1$_{386-405}$, only *PARK2*$^{-/-}$ exhibited symptoms resembling EAE. During the acute phase, *PARK2*$^{-/-}$ mice immunized with either MOG$_{35-55}$ or EBNA1$_{386-405}$ exhibited similar infiltration of T cells and macrophages in the spinal cord and decreased GFAP expression in the brain. However, EBNA1$_{386-405}$ -immunized *PARK2*$^{-/-}$ mice showed significantly increased frequencies of CD8a+ T cells and CD11c+ B cells, and distinct cytokine profiles in the periphery compared to wild-type controls. These findings highlight the role of EBV in exacerbating inflammation, particularly in the context of mitochondrial deficiencies.

Keywords: Epstein-Barr virus; PARK2 knockout mice; mitochondrial dysfunction; experimental autoimmune encephalomyelitis; neuroinflammation

1. Introduction

The exact cause of autoimmune responses in neuroinflammatory disorders like multiple sclerosis (MS) remains unclear. While certain genetic variations increase the risk, they do not guarantee disease onset. Environmental factors, including infections, significantly contribute to the development of central nervous system (CNS) inflammatory disorders such as MS [1]. However, direct evidence of a specific pathogenic agent causing MS is still lacking.

Epstein-Barr virus (EBV), a member of herpes virus family which establishes latent infection with periodic reactivation, is considered a potential environmental trigger in MS development, possibly by infecting B cells [2]. Research shows a correlation between prior EBV infection and an increased risk of MS onset [3]. This suggests that molecular mimicry, where EBV antigens resemble self-antigens, may induce autoimmunity in genetically susceptible individuals [4]. Given that over 90% of the global population is seropositive for EBV [5], other factors such as interactions with additional pathogens, vaccination profiles, and specific genetic variations likely contribute to the

 doi:10.20944/preprints202408.1776.v1

difference in MS prevalence between high- and low-risk areas. These factors can also influence the highly heterogeneous disease course.

Mitochondrial dysfunctions play an important role in the progression of neurological disorders, including MS, contributing to energy deficiency, oxidative stress, inflammation, and neurodegeneration [6]. Reduced ATP production due to mitochondrial dysfunctions can weaken the immune system, causing metabolic dysfunction in peripheral immune cells [7]. In MS, demyelinated axons require more energy to propagate action potentials, and mitochondrial dysfunction exacerbates the energy deficit, further compromising neuronal function.

Infections can impact mitochondrial function, and conversely, mitochondrial dysfunction can influence the body's ability to respond to infections [8]. Infections can lead to increased production of reactive oxygen species and the release of cytokines, disrupting mitochondrial dynamics [9]. This bidirectional relationship between mitochondrial dysfunction and infections highlights the complex interplay contributing to the pathogenesis of MS and other neuroinflammatory disorders.

Mitophagy, a selective form of autophagy that target damaged or dysfunctional mitochondria for degradation and recycling, plays a crucial role in the host's defense against infections by maintaining mitochondrial quality, regulating immune responses, and preventing excessive inflammation [10]. One of the most well-characterized pathways for mitophagy is the PTEN-induced putative kinase 1 (PINK1)-Parkin Pathway [11]. In this pathway, PINK1 accumulation on damaged mitochondria recruits and activates Parkin (encoded by the *PARK2* gene), leading to the ubiquitination of mitochondrial proteins and the recruitment of autophagy receptors [11]. Notably, mutations in PINK1, Parkin, and other mitophagy-related proteins are linked to early-onset Parkinson's disease [11].

Recent research has demonstrated that PINK1 and Parkin are also associated with mechanisms related to innate and adaptive immunity in the context of neuroinflammation and neurodegeneration. For instance, intestinal infection with Gram-negative bacteria in *PINK1* knockout mice triggers mitochondrial antigen presentation and autoimmune mechanisms, leading to the establishment of cytotoxic mitochondria-specific CD8 T cells in both the periphery and the brain [12]. Furthermore, the absence of PINK1 and Parkin proteins exacerbates acute inflammation in active experimental autoimmune encephalomyelitis (EAE) with myelin oligodendrocyte glycoprotein (MOG) in C57BL/6J mice [13,14]. Both proteins have an age-related influence on various subsets of innate and adaptive immune cells in the periphery and CNS at different stages of active EAE progression [13,14]. This age-related impact suggests that the functional roles of PINK1 and Parkin in immune modulation and neuroprotection may vary over the lifespan, affecting the severity and progression of neuroinflammatory conditions such as MS and other neurodegenerative diseases.

To investigate the relationship between altered mitophagy, EBV, and neuroinflammation, we analyzed the impact of immunization with a recently discovered peptide from the EBV nuclear antigen EBNA1 that cross-reacts with glial cell adhesion protein (GlialCAM) in the CNS [15]. This study was conducted in both *PARK2* knockout (*PARK2*$^{-/-}$) and wild-type mice, and the results were compared with those from immunization using the MOG-EAE model in the same mice. Our study demonstrated that alterations in mitochondria-mediated immune responses lead to increased inflammation due to the EBV antigenic component. This suggests that EBV peptides might exacerbate neuroinflammation through molecular mimicry and mitochondrial dysfunction, highlighting the potential for targeted therapeutic strategies that address these specific immune and mitochondrial pathways in neuroinflammatory diseases like MS.

2. Results

2.1. EAE Progression and Immunization Response in PARK2$^{-/-}$ *and Wild-Type Mice*

Firstly, we compared the clinical progression of EAE between middle-aged *PARK2*$^{-/-}$ and wild-type mice. Our findings confirmed that the absence of *PARK2*$^{-/-}$ significantly exacerbates the severity of EAE, consistent with previous observations in young mice [13]. The peak disease score was significantly higher in *PARK2*$^{-/-}$ mice (3.6 ± 0.5) compared to wild-type controls (3.0 ± 0.5) ($p < 0.0005$)

 doi:10.20944/preprints202408.1776.v1

(Figure 1A). Additionally, *PARK2*$^{-/-}$ mice demonstrated delayed recovery 30 days post-immunization. Both groups exhibited similar incidence, mortality, and disease onset (Table 1). All mice exhibited experienced a significant reduction in body weight during the first 10 days after immunization, with the weight loss remaining significant in *PARK2*$^{-/-}$ mice up to 30 days post-immunization (Figure 1B).

Next, we analyzed the effect of EBNA1$_{386–405}$ immunization, which revealed notable differences in clinical scores between *PARK2*$^{-/-}$ and wild-type mice (Figure 1D). Notably, only *PARK2*$^{-/-}$ mice displayed symptoms like EAE, including limp tail, limb weakness, and occasional partial paralysis of the hind limbs. When comparing *PARK2*$^{-/-}$ mice immunized with MOG$_{35–55}$ or EBNA1$_{386–405}$, the latter group exhibited a delayed onset (12 ± 1.4 days *vs* 16 ± 1.4, $p < 0.0001$), reduced severity, and improved recovery 30 days post-immunization (Table 1). All wild-type mice immunized with EBNA1$_{386–405,}$ even exhibited similar body weight changes during the first 10 days post immunization compared to *PARK2*$^{-/-}$ mice (Figure 1E). However, after this period, weight recovery in the wild-type mice was associated with the absence of any neurological signs typical of EAE. Clinical characteristics of all mice are reported in Table 1.

Regarding T cell proliferation during the acute phase, preliminary assays indicated that both MOG$_{35-55}$ and EBNA1$_{386–405}$, at a final concentration of 50 mg/mL, had the strongest stimulatory effect on CD3^{+} T cells, whit their percentage in the spleen ranged from a mean of 15% to 30%. In middle-aged *PARK2*$^{-/-}$ mice, stimulation with either MOG$_{35-55}$ (Figure 1C) or EBNA1$_{386–405}$ (Figure 1F) significantly enhanced T lymphocyte proliferation compared to wild-type mice, with a notably stronger stimulatory effect ($p < 0.0001$ and $p = 0.0002$, respectively).

Table 1. Clinical difference between *PARK2*$^{-/-}$ and C57BL/6J wild-type mice immunized with MOG$_{35-55}$ or EBNA1$_{386-405.}$

	MOG$_{35-55}$ immunization		**EBNA1$_{386-405}$ immunization**	
N=20 x group	*PARK2*$^{-/-}$	C57BL/6J	*PARK2*$^{-/-}$	C57BL/6J
Incidence	90%	90%	40% *	0%
Mortality	10%	5%	0%	0%
Onset	12 ± 1.4	13 ± 1.5	16 ± 1.4 *	-
Peak	3.6 ± 0.5 *	3.0 ± 0.6	2 ± 1 *	-

* Statistically significant when comparing knockout and wild-type mice with the same immunization.

 doi:10.20944/preprints202408.1776.v1

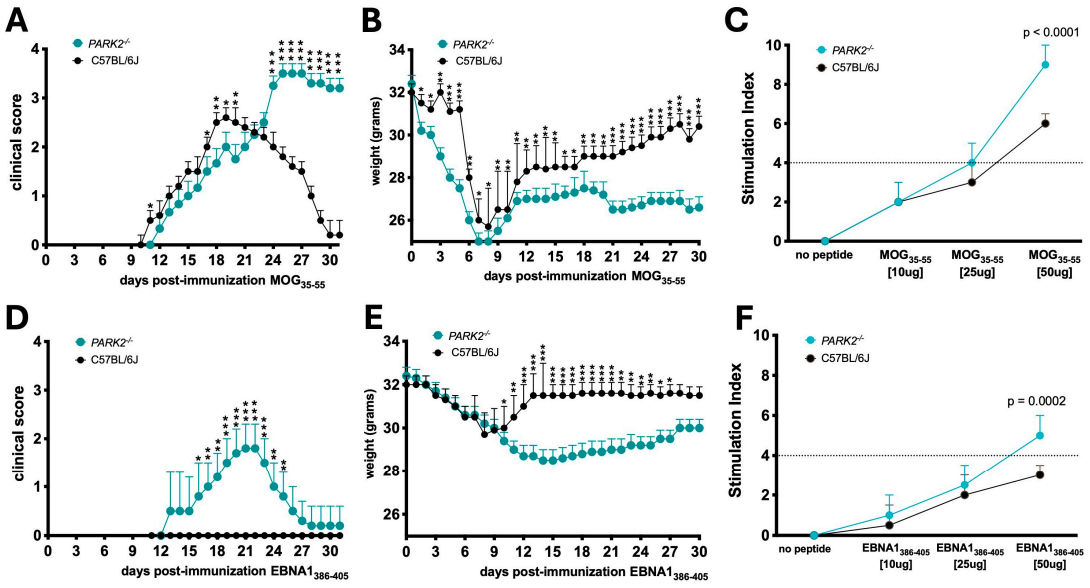

Figure 1. Comparison of disease progression after EBNA1$_{386-405}$ or myelin oligodendrocyte glycoprotein (MOG)$_{35–55}$ immunization between *PARK2*$^{-/-}$ and C57BL/6J mice. Clinical scores and body weights in mice induced by active EAE (**A, B**) or in mice immunized with the EBNA1$_{386-405}$ peptide **(D, E)**. Combined results from three independent experiments, with 20 mice per group. T-cell proliferative response to MOG$_{35–55}$ peptide **(C)** or to EBNA1$_{386-405}$ peptide **(F)**. The data show one experiment with 5 mice per group of three independent. Statistical analyses were performed by two-way analysis of variance (ANOVA). * $p < 0.05$; ** $p < 0.01$; $p < 0.001$.

2.2. Differential Peripheral Immune Cell Populations and Cytokine Profiles in PARK2$^{-/-}$ *Mice Following EBNA1-Immunization and EAE Induction*

Peripheral cells were isolated from the spleens of mice 20 days after immunization with either the antigenic peptides or PBS (placebo control) and analyzed using cytofluorimetry (Figure 2A). No differences were observed in peripheral immune cell populations between PBS-immunized *PARK2*$^{-/-}$ mice and PBS-immunized wild-type mice (data not shown).

In middle-aged MOG$_{35-55}$-immunized mice, *PARK2*$^{-/-}$ mice exhibited significantly higher levels of both CD4$^+$ ($p = 0.002$) and CD8$^+$ ($p = 0.04$) T cells compared to wild-type controls during the acute disease phase of EAE (Figure 2B1). The percentage of of B cells did not differ between the groups (Figure 2B2)

In EBNA1$_{386-405}$-immunized mice, *PARK2*$^{-/-}$ mice had a higher percentage of CD8$^+$ T cells ($p = 0.01$) (Figure 2B3) and CD11c$^+$ CD19$^+$ B cells ($p = 0.02$) (Figure 2B4) compared to wild-type mice, which did not develop any disease symptoms.

When comparing *PARK2*$^{-/-}$ mice immunized with MOG$_{35-55}$ to those immunized with EBNA1$_{386-405}$, there were significant differences in the percentage of CD4$^+$ T lymphocytes ($p < 0.0001$) (Figure 2C1), but no differences in CD8$^+$ T lymphocytes (Figure 2C2). Additionally, EBNA1$_{386-405}$-immunized mice showed the highest percentage of CD11c$^+$ B cells($p = 0.0002$) (Figure 2C3).

Cytokine profiling of spleen cells from middle-aged mice immunized with MOG$_{35-55}$ peptide revealed a significant increase in IL-17 levels in *PARK2*$^{-/-}$ mice compared to wild type controls during the acute disease phase of EAE ($p = 0.02$) (Figure 2D1). In contrast, EBNA1$_{386-405}$-immunized *PARK2*$^{-/-}$ mice exhibited significantly higher expression of IL-6 ($p = 0.004$), interferon gamma (IFN-γ) ($p = 0.02$) and particularly tumor necrosis factor-α (TNF-α) ($p < 0.001$) compared to wild type mice (Figure 2D2).

 doi:10.20944/preprints202408.1776.v1

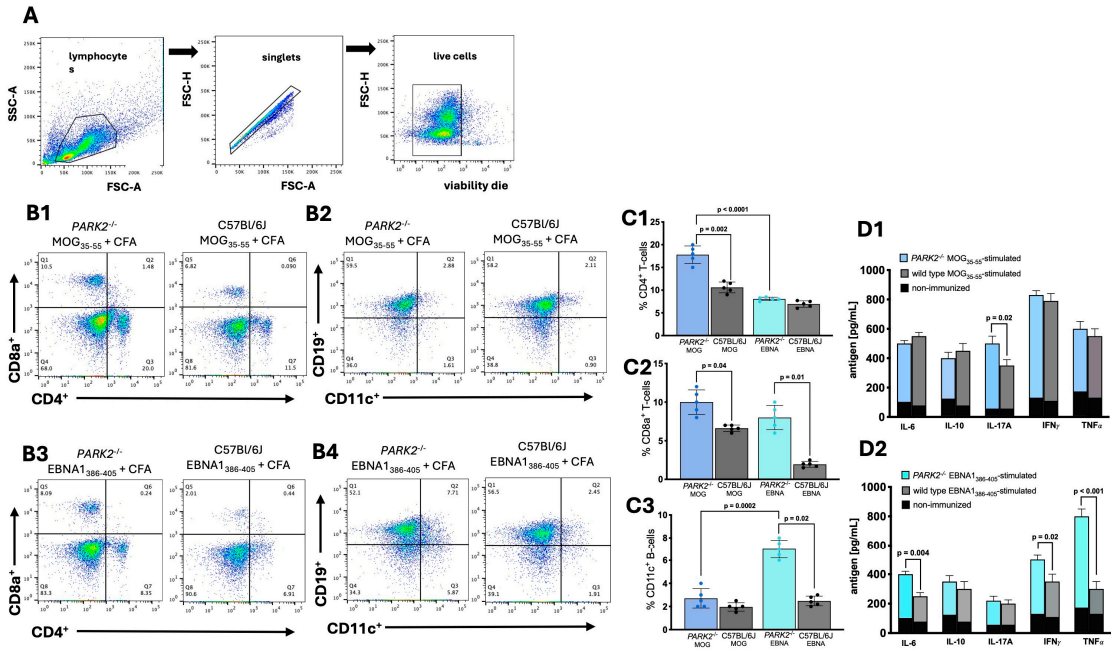

Figure 2. Immune cell populations and cytokine profiles in splenocytes from *PARK2*$^{-/-}$ and wild-type mice 20 days post-immunization. Gating strategy for flow cytometry. (A). Representative plots showing CD8^{+} and CD4^{+} T-cells (B1, B3), and CD11c^{+} CD19^{+} B-cells (B2, B4), along with corresponding graphs (C1-C3). Cytokine expression profiles in culture supernatants of splenocytes stimulated with MOG$_{35-55}$, EBNA$_{386-405}$, or non-immunized (D1, D2). The data represent a single c experiment with N = 5 mice per group, as part of three independent experiments. Results are.

2.3. Increased Inflammatory Cell Infiltration in Spinal Cords of PARK2$^{-/-}$ *Mice Following Immunization with MOG*$_{35-55}$ *and EBNA11*$_{386-405}$ *Peptides*

We analyzed the spinal cords of mice isolated at day 20 during the acute phase using immunohistochemistry. No cell infiltration was detected in the spinal cords of non-immunized control mice. In the spinal cords of *PARK2*$^{-/-}$ mice immunized with MOG$_{35-55}$ to induce EAE, we observed significantly higher inflammatory infiltration ($p = 0.0003$) (Figure 3A1) compared to wild-type controls with EAE (Figure 3A2). Following immunization with the EBNA1$_{386-405}$ peptide, *PARK2*$^{-/-}$ mice, which developed a clinical presentation resembling classic EAE, showed typical inflammatory cell infiltration in the spinal cord (Figures 3A3). In contrast, no inflammatory cell infiltration was observed in the spinal cord tissue of wild-type control mice (Figure 3A4). When comparing *PARK2*$^{-/-}$ mice immunized with MOG$_{35-55}$ and EBNA11$_{386-405}$ peptides, the former showed a statistically significant decrease in overall inflammation ($p = 0.001$) (Figure A5).

The inflammatory infiltration was primarily composed of CD3^{+} T cells (Figure 3B1-B5), CD68^{+} monocytes (Figure 3C1-C5), and TMEM119^{+} microglia (Figure 3D1-D5). Immunohistochemistry also revealed a significantly increased number of CD3^{+} T cells in *PARK2*$^{-/-}$ mice immunized with MOG$_{35-55}$ also showed a significant percentage of CD3^{+} T cells compared to *PARK2*$^{-/-}$ mice immunized with EBNA1$_{386-405}$ peptide ($p = 0.05$) (Figure 3B5).

presented as mean ± standard deviation, analyzed using Kruskal-Wallis test.

 doi:10.20944/preprints202408.1776.v1

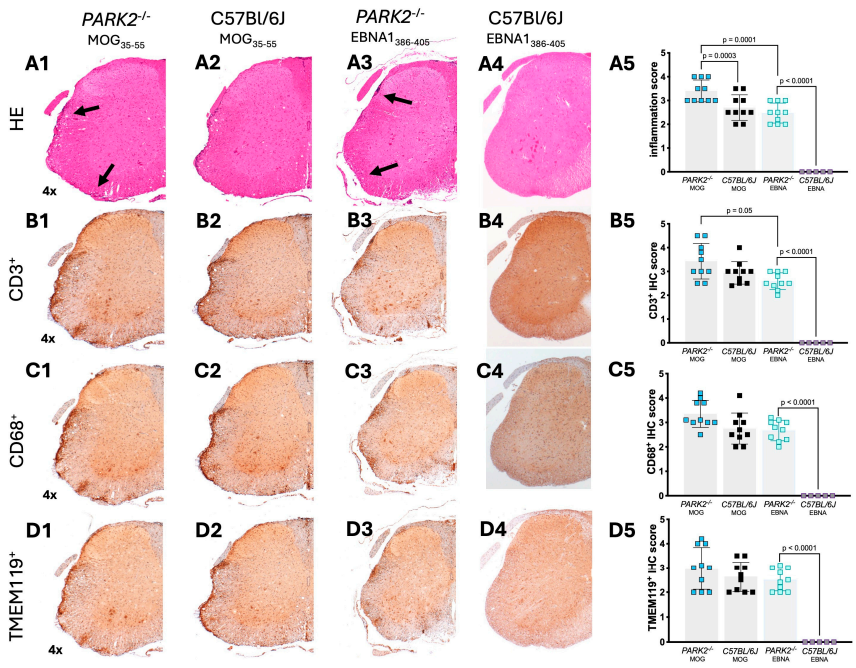

Figure 3. Histological analysis of inflammatory infiltration in spinal cord of *PARK2*$^{-/-}$ and C57BL/6J mice during the acute disease phase. The histological images show sections (scale bar = 200 um) of the lumbar spinal cord from *PARK2*$^{-/-}$ and C57BL/6J wild-type mice after immunization with MOG$_{35-55}$ or EBNA1$_{386-405}$ peptides. These images highlight inflammatory cell infiltration (Hematoxylin and Eosin staining) (A1-A5), the presence of infiltrated CD3^{+} T cells (B1-B5) and CD68^{+} macrophages/monocytes (C1-C5), and the expression of TMEM119^{+} microglia (D1-D5) in the white matter. For the semi quantitative analysis of mice, stain-positive cells were counted across two randomly selected sections from ten mice in each group. Arrows indicate areas with inflammatory infiltrates. Data were analyzed using Kruskal-Wallis test.

2.4. Different Density of GFAP^{+} Cells in the Hippocampus of PARK2$^{-/-}$ Mice during Inflammation

Previous studies have shown different density of GFAP^{+} cells in *PARK2*$^{-/-}$ mice during inflammation [13]. Based on these findings, we focused our analysis on the hippocampal region of mice immunized with MOG$_{35-55}$ or EBNA1$_{386-405}$ peptides. GFAP^{+} cells did not significantly differ between *PARK2*$^{-/-}$ and C57BL/6J wild-type mice with non-immunization [13]. However, immunofluorescence staining revealed a significant reduction in GFAP^{+} cells across various hippocampal regions in *PARK2*$^{-/-}$ mice compared to wild-type mice during the acute disease phase of EAE ($p = 0.001$) (Figure 4A). In *PARK2*$^{-/-}$ mice immunized with the EBNA1$_{386-405}$ peptide that developed EAE-like symptoms, the number of GFAP^{+} cells was also reduced compared to C57BL/6J controls (Figure 4B), though this reduction was less pronounced than in *PARK2*$^{-/-}$ mice immunized with MOG$_{35-55}$.

 doi:10.20944/preprints202408.1776.v1

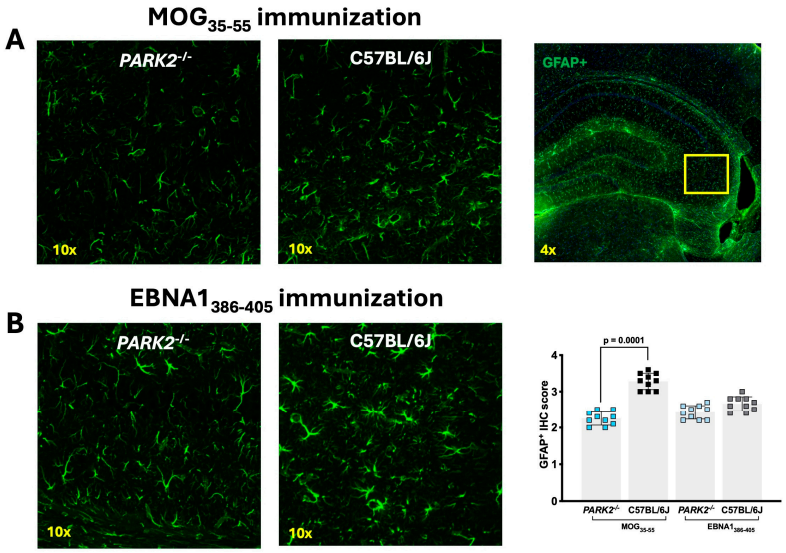

Figure 4. Confocal fluorescence microscopy of GFAP labeled brain tissue from *PARK2*$^{-/-}$ and C57BL/6J mice immunized with MOG$_{35-55}$ or EBNA1$_{386-405}$ peptides during the acute disease phase. The panels show sections (scale bar = 200 um) of hippocampus from *PARK2*$^{-/-}$ and C57BL/6J wild-type mice after immunization with MOG$_{35-55}$ (A) or EBNA1$_{386-405}$ peptides (B). GFAP^{+} cells were semi-quantitatively analyzed by counting across two randomly selected sections from ten mice in each group. Data were analyzed using Kruskal-Wallis test.

3. Discussion

In this study, we confirmed the role of Parkin protein in modulating peripheral immune cells-mediated immunity during EAE, and the role of EBV in neuroinflammation within the context of mitochondrial dysfunctions. Specifically, we demonstrated that subcutaneously immunization with the immunogenic peptide EBNA1$_{385-405}$ in adjuvant, along with pertussis toxin administration, can induce symptoms consistent with active MOG-EAE in middle-aged female *PARK2*$^{-/-}$ mice, which exhibit mitochondrial dysfunctions involved in mitophagy.

A previous study showed that young *PARK2*$^{-/-}$ mice experienced more severe EAE disease and an earlier onset compared to wild-type controls, characterized by a high frequency of CD8^{+} T cells in the periphery and brain [13]. This indicates that mitochondrial dysfunctions influence the course of MOG-EAE-induced neuroinflammation in mice with a C57Bl/6J genetic background. Another recent study highlighted that EBNA1$_{386-405}$ is involved in high-affinity molecular mimicry with the CNS protein GlialCAM, revealing cross-reactive anti-EBNA1 and anti-GlialCAM antibodies in patients with MS [15]. Additionally, this study showed that young SJL/J mice immunized with the EBNA1$_{386-405}$ peptide a few weeks before inducing active EAE with myelin proteolipid protein (PLP)$_{139-151}$ developed more severe EAE in terms of symptoms, CNS immune cell infiltration, and demyelination [15]. EBNA1$_{385-405}$ also stimulated the secretion of B cell stimulatory T helper cytokines and a strong CD4 response [15].

Our study confirms the encephalitogenic role of EBNA1$_{386-405}$ but with several key differences. Firstly, only *PARK2*$^{-/-}$ mice developed symptoms similar to EAE, not wild-type mice. We did not evaluate the effect of EBNA1$_{386-405}$ before or after MOG-EAE immunization or the effect of a boost. Instead, we assessed the direct immunization effect of EBNA1$_{386-405}$ and compared it to MOG-EAE.

In our model, *PARK2*$^{-/-}$ mice immunized with EBNA1$_{386-405}$ exhibited a significant percentage of CD8^{+} cells in the periphery compared to C57Bl/6J wild-type controls that did not develop any symptoms. The Parkin protein encoded by *PARK2* regulates adaptive immunity by repressing mitochondrial antigen presentation [16]. The absence of Parkin can promote the establishment of peripheral mitochondrial antigen-specific T cell populations, which can access the CNS during infections or neuroinflammation [16]. Interestingly, studies investigating anti-EBV immunity in the

 doi:10.20944/preprints202408.1776.v1

CNS of MS patients suggest that EBV-specific T cells gain access to the brain and that altered intrathecal CD8 T cell responses toward EBV could contribute to CNS inflammation and tissue damage [17].

We also observed an increased frequency of $CD11C^+CD19^+$ B cells in the periphery of *PARK2*$^{-/-}$ mice immunized with $EBNA1_{386-405}$ compared to wild-type controls [18]. These cells, primarily memory B cells prone to differentiate into antibody secreting cells [19], continuously expands with age in healthy individuals but show a premature and pronounced accumulation in autoimmune diseases [18]. It has been suggested that these age-related cells are functional mediators of viral-enhanced autoimmunity, as they increase during latent viral infections [18]. The latent form of EBV appears to prime $CD11C^+CD19^+$ B cells, contributing pathogenically to autoimmune diseases [20,21].

Interestingly, *PARK2*$^{-/-}$ mice immunized with MOG_{35-55} showed in the periphery elevated concentrations of the key Th17 cytokine IL-17A during the acute phase compared to wild-type control. In contrast, *PARK2*$^{-/-}$ mice immunized with $EBNA1_{386-405}$ exhibited lower IL-17A levels but higher concentration of IL-6, IFN-γ and TNF-α. Notably, TNF-α was also elevated in *PARK2*$^{-/-}$ mice immunized with $EBNA1_{386-405}$ compared to those immunized with MOG_{35-55}. These findings partially align with previously studies, which demonstrated that $EBNA1_{386–405}$ stimulated the secretion of IFN-γ, TNF, and IL-12, as well as IL-6 and IL-10, while suppressing IL-17 [15].

Notably, we observed a reduced number of $GFAP^+$ cells in the hippocampus of *PARK2*$^{-/-}$ compared to wild-type mice, regardless of MOG_{35-55} or $EBNA1_{386-405}$ immunization. While $GFAP^+$ cells in the hippocampus are primarily associate with astrocytes, they may also include neuronal precursor cells, as embryonic $GFAP^+$ cells in young adult mice predominantly differentiate into neurons rather than astrocytes [22]. This reduction in $GFAP^+$ cells could potentially compromise the integrity of the blood-brain barrier, increasing the brain's vulnerability to pathogens, and may also negatively affect neurological recovery.

Another difference is that we selected 9-month-old mice for this study. This age represents a middle-aged mouse, typically extending from 8 to 15 months [23], corresponding approximately 35 years in humans. MS onset usually occurs in women between 20-40 years, with an average onset at 35 years. Moreover, a significant proportion of people with MS experience progression independent of relapse activity (PIRA) followed by post-inflammatory neurodegenerative processes over the years. The first attack of PIRA MS usually occurs at an average age of 32 years [24].

We hypothesize that progressing mitochondrial dysfunction, associated with aging [25], and EBV infection could be pathological drivers in progressive forms of MS, transiently exacerbating pre-existing symptoms. To test this hypothesis, we require a chronic model of EAE, as our current model induces only a monophasic form of EAE. Additionally, we need to investigate the presence of EBV markers by directly analyzing body fluids from patients with PIRA or progressive forms of MS.

Unbalanced mitochondrial activity is involved in inflammation in several neurological diseases [26]. It is important to note that our studies used *PARK2*$^{-/-}$ mice, which have mutations related to Parkinson's disease [11]. Despite exhibiting different clinical profiles, common mechanisms related to neurodegeneration, such as mitochondrial dysfunctions, are observed in patients with Parkinson 'disease and MS, suggesting converging pathogenic pathways of neurodegeneration. Several cases of co-occurrence of PD after diagnosis of MS have been reported [27], including a patient with early-onset Parkinson's disease and a heterozygous PARK2 mutation who after 8 years developed primary progressive MS [28]. Moreover, the detection of significantly increased levels of Parkin protein in the peripheral blood and cerebrospinal fluids of patients with MS [29,30] indicates a potential role for Parkin in the pathogenesis of MS.

Abnormalities in mitochondria are related to dysfunctional response to infection [31]. Conversely, EBV-encoded proteins during both the latency and lytic infection reduce autophagy, decrease intracellular reactive oxygen species, and modulate mitochondrial function, altering bioenergetics [32]. Clinical and in-vitro evidences associates EBV to Parkinson's disease and the occurrence of parkinsonism [33], with virus-mediated cell-cycle dysregulation potentially initiating neurodegenerative processes [34]. However, further studies are needed to clarify the precise role of EBV. For instance, one limitation of our study is that our data were obtained from experiments

 doi:10.20944/preprints202408.1776.v1

conducted on female mice. Although previously published data indicate no differences in the development of EAE between male and female *PARK2*$^{-/-}$ mice [13,14], our findings are restricted to the monophasic EAE model during the effector phase of the disease. Given that in MS, sex differences influence disease pathogenesis, such as men accumulating disability more rapidly than women [35], future research should focus on the recovery phase, utilizing progressive EAE models. In this context, there may be significant differences between male and female mice. Another area for investigation is the impact of mycobacterial components, such as CFA, on the development of EAE in *PARK2*$^{-/-}$ mice. Literature indicates that CFA administration can induce mild neuroinflammation [36] and that immunization with mycobacterial components can modulate EAE development [37]. Therefore, it would be interesting to evaluate the effects of CFA alone and other mycobacterial components in our model, particularly in the context of mitochondrial dysfunctions.

Despite areas requiring further clarification, our study demonstrated that alterations in mitochondria-mediated immune responses lead to increased inflammation triggered by the EBV antigenic component. This suggests that EBV peptides may exacerbate neuroinflammation through mechanism of molecular mimicry and mitochondrial dysfunction. These findings highlight the potential for developing targeted therapeutic strategies that significantly address these immune and mitochondrial pathways in neuroinflammatory diseases like MS.

4. Materials and Methods

4.1. Generation and Maintenance of PARK2$^{-/-}$ *Mice*

PARK2$^{-/-}$ middle-aged (9 months old) female mice (N=20 / group) were generated at Juntendo University [38]. A targeting vector was constructed with 1.5- and 7-kb DNA fragments serving as the 5′ and 3′ homologous sequences, respectively. A negative selection cassette, DTA, encoding diphtheria toxin, was also included. The linearized targeting vector was transfected into TT2 ES cells, and clones were selected in G418. Screening for homologous recombination was done by Southern blotting, using a 5′ external probe and a neo-specific probe, confirming the desired recombination in the clones. ES cells from these clones were injected into C57BL/6J embryos, and chimeric offspring were crossed with C57BL/6J mice to achieve germline transmission, verified by Southern analysis with the 5′ probe. Heterozygous mice were interbred to produce homozygous knockout mice and wild-type littermate, which were sex-and aged-matched as controls. We chose female mice because previous experiments demonstrated that both knockout and wild-type young (8-12 weeks old) female mice have high susceptibility to EAE induction [13]. Animals were housed in a pathogen-free facility, maintained under a 12-12-hour light/dark cycle. Procedures were approved by the Animal Experimental Committee of the Juntendo University Graduate School of Medicine (approved protocol no. 290238) and conducted in accordance with NIH and Juntendo University guidelines.

4.2. Immunization and Monitoring of PARK2$^{-/-}$ *and Wild-Type Mice*

Peptides EBNA1$_{386-405}$ (sequence CSQSSSSGSPPRRPPPGRRPF), derived from the EBNA1 protein (UniProt accession number P03211), and MOG$_{35-55}$ (sequence MEVGWYRSPFSRVVHLYRNGK) were chemically synthesized to a purity exceeding 95% by Synpeptide Co, Shanghai, China.

A cohort of *PARK2*$^{-/-}$ and wild-type mice were subcutaneously immunized with either 200 µg of EBNA1$_{386-405}$ peptide or with 200 µg of the MOG$_{35-55}$ peptide, both emulsified in incomplete Freund's adjuvant (BD Diagnosis) supplemented with *Mycobacterium tuberculosis* H37Ra (Difco, Detroit, MI, USA) at a final concentration of 4mg/mL. Pertussis toxin (200 ng) (Difco) was administrated intraperitoneally to all mice at the time of immunization and 48 h post-immunization. All mice were monitored daily, and disease severity was assessed using the following criteria: 0, no clinical signs; 1, flaccid tail; 2, mild hind limb weakness; 3, severe hind limb weakness; 4, hind limb paralysis; 5, moribund state or death.

4.3. Assessment of T Cell Proliferation Using ^{3}*H-Thymidine Incorporation in MOG*$_{35-55}$ *and EBNA1*$_{386-405}$ *Immunized Mice*

 doi:10.20944/preprints202408.1776.v1

For the T cell proliferation assay, $CD3^+$ T cells were isolated and purified by immunomagnetic positive selection from the spleens of mice immunized with either $MOG_{35–55}$ or $EBNA1_{386-405}$ using the MojoSort Mouse CD3 Cell Isolation Kit (BioLegend). T cells (4 x 10^5 cells/well) were cultured for 2 days with 50 μg/mL of the specific peptide. This was done in the presence of gamma-irradiated (3000 rad) accessory spleen cells, which were syngeneic to the responding T cells, at a concentration of 1 x 10^6 cells/ml. Cell proliferation during the last 18 hours was measured by determining the radioactivity of incorporated-3H-thymidine (PerkinElmer, Waltham, MA, USA) using a microplate scintillation counter (MicroBeta TriLux, PerkinElmer). The proliferative response was expressed as a stimulation index (counts per minute [cpm] of cells with test peptides/cpm of cells without stimulation) from triplicate determinations.

4.4. Cytofluorimetric Analysis of Spleen Cells

For cytofluorimetric analysis, spleen cell single-cell suspensions ($1x10^6$ cells) were labeled with live/dead markers (Zombie NIR Fixable Viability Kit, Biolegend, USA) for 15 min at room temperature, followed by a 10-minutes preincubation with FcBlock (FcγRII-RIII) on ice. Afterward, the cells were stained on ice for 20 min with fluorochrome-labeled monoclonal antibodies targeting CD4 (GK1.5), CD8a (53-6.7], CD19 (1D3), CD11c (N418), CD5 (53.7.3), Ly6G (1A8), CD11b (M1/70), CD115 (AFS98), I-A/I-E (M5/114.15.2), all purchased from Biolegend, or performed with appropriate isotype-matched controls. Sample acquisition (20000 events/sample) was performed on a BD FACSCelesta™ (BD Biosciences, USA), and data was analysis conducted using FlowJo software version 10.10.0 (FlowJo Company).

4.5. Cytokine Profiling Following Antigen-Specific T-Cell Stimulation

Spleen cells were isolated from all mice 20 days post immunization and incubated with either MOG_{35-55} or $EBNA1_{386-405}$ for 48 hours, following previously established protocols [13,14]. Cytokine concentrations in the culture supernatants were then measured using a multi-analyte ELISArray kit (Qiagen, Hilden, Germany), according to the manufacturer's instructions.

4.6. Histology and Immunohistochemical Analysis of Mice Tissues

Mice were transcardially perfused with PBS followed by 4% paraformaldehyde (PFA) in PBS. The brains and spinal cords were then post-fixed in 4% PFA and embedded for sectioning. Paraffin-embedded tissue sections were stained with Hematoxylin/Eosin to evaluate inflammation, quantified as the percentage of infiltrated area over the total spinal cord sections.

Immunohistochemistry and immunofluorescence were performed as previously described [14], utilizing primary antibodies against CD3 (1:100), CD68 (1:500), glial fibrillary acidic protein (GFAP) (1:1000), and transmembrane protein 119 (TMEM119) (1:300), all obtained from Abcam, Tokyo, Japan. These were followed by incubation with appropriate biotinylated or fluorescent secondary antibodies. All samples were processed simultaneously to ensure comparability, and results were quantified using a previously established semi-quantitative scoring system [14].

4.7. Statistical Analysis

Statistical analysis was conducted using GraphPad Prism version 10.2.3 (GraphPad Software, La Jolla, CA, USA). Clinical scores, body weights, and T cell proliferation data were analyzed using two-way analysis of variance (ANOVA). Flow cytometry, cytokine assays, and histological data were assessed with the Kruskal-Wallis non-parametric test followed by Dunn's post hoc analysis. A p-value of less than 0.05 was considered statistically significant.

Author Contributions: Conceptualization, D.C.; Methodology, D.C., Y.T., S.N., E.M., T.S., H.O.; writing, D.C.; supervision, K.Y., L.A.S., N.H.; funding acquisition, D.C. All authors have read and agreed to the published version of the manuscript.

Funding: This research was funded by JSPS KAKENHI Grant Number 23K14675 to D.C., and PRIN 2022 Grant Number 202238WEHT to D.C.

Institutional Review Board Statement: All animal research was performed in accordance with the Proper Conduction of Animal Experiments of the Institutional Animal Care and Use Committee of Juntendo University (approved protocol no. 290238).

Data Availability Statement: The data underlying this article will be shared on reasonable request to the corresponding author.

Conflicts of Interest: The authors declare no conflict of interest.

References

1. Steelman, A.J. Infection as an Environmental Trigger of Multiple Sclerosis Disease Exacerbation. *Front Immunol* **2015**, *6*, 520, doi:10.3389/fimmu.2015.00520.
2. Soldan, S.S.; Lieberman, P.M. Epstein-Barr virus and multiple sclerosis. *Nat Rev Microbiol* **2023**, *21*, 51-64, doi:10.1038/s41579-022-00770-5.
3. Bjornevik, K.; Munz, C.; Cohen, J.I.; Ascherio, A. Epstein-Barr virus as a leading cause of multiple sclerosis: mechanisms and implications. *Nat Rev Neurol* **2023**, *19*, 160-171, doi:10.1038/s41582-023-00775-5.
4. Dempsey, L.A. Molecular mimicry in MS. *Nat Immunol* **2022**, *23*, 343, doi:10.1038/s41590-022-01156-8.
5. Dunmire, S.K.; Verghese, P.S.; Balfour, H.H., Jr. Primary Epstein-Barr virus infection. *J Clin Virol* **2018**, *102*, 84-92, doi:10.1016/j.jcv.2018.03.001.
6. Barcelos, I.P.; Troxell, R.M.; Graves, J.S. Mitochondrial Dysfunction and Multiple Sclerosis. *Biology (Basel)* **2019**, *8*, doi:10.3390/biology8020037.
7. Wang, P.F.; Jiang, F.; Zeng, Q.M.; Yin, W.F.; Hu, Y.Z.; Li, Q.; Hu, Z.L. Mitochondrial and metabolic dysfunction of peripheral immune cells in multiple sclerosis. *J Neuroinflammation* **2024**, *21*, 28, doi:10.1186/s12974-024-03016-8.
8. Tiku, V.; Tan, M.W.; Dikic, I. Mitochondrial Functions in Infection and Immunity. *Trends Cell Biol* **2020**, *30*, 263-275, doi:10.1016/j.tcb.2020.01.006.
9. Manoharan, R.R.; Prasad, A.; Pospisil, P.; Kzhyshkowska, J. ROS signaling in innate immunity via oxidative protein modifications. *Front Immunol* **2024**, *15*, 1359600, doi:10.3389/fimmu.2024.1359600.
10. Cho, D.H.; Kim, J.K.; Jo, E.K. Mitophagy and Innate Immunity in Infection. *Mol Cells* **2020**, *43*, 10-22, doi:10.14348/molcells.2020.2329.
11. Hattori, N.; Saiki, S.; Imai, Y. Regulation by mitophagy. *Int J Biochem Cell Biol* **2014**, *53*, 147-150, doi:10.1016/j.biocel.2014.05.012.
12. Matheoud, D.; Cannon, T.; Voisin, A.; Penttinen, A.M.; Ramet, L.; Fahmy, A.M.; Ducrot, C.; Laplante, A.; Bourque, M.J.; Zhu, L.; et al. Intestinal infection triggers Parkinson's disease-like symptoms in Pink1(-/-) mice. *Nature* **2019**, *571*, 565-569, doi:10.1038/s41586-019-1405-y.
13. Cossu, D.; Yokoyama, K.; Sato, S.; Noda, S.; Sechi, L.A.; Hattori, N. PARKIN modifies peripheral immune response and increases neuroinflammation in active experimental autoimmune encephalomyelitis (EAE). *J Neuroimmunol* **2021**, *359*, 577694, doi:10.1016/j.jneuroim.2021.577694.
14. Cossu, D.; Yokoyama, K.; Sato, S.; Noda, S.; Sakanishi, T.; Sechi, L.A.; Hattori, N. Age related immune modulation of experimental autoimmune encephalomyelitis in PINK1 knockout mice. *Front Immunol* **2022**, *13*, 1036680, doi:10.3389/fimmu.2022.1036680.
15. Lanz, T.V.; Brewer, R.C.; Ho, P.P.; Moon, J.S.; Jude, K.M.; Fernandez, D.; Fernandes, R.A.; Gomez, A.M.; Nadj, G.S.; Bartley, C.M.; et al. Clonally expanded B cells in multiple sclerosis bind EBV EBNA1 and GlialCAM. *Nature* **2022**, *603*, 321-327, doi:10.1038/s41586-022-04432-7.
16. Matheoud, D.; Sugiura, A.; Bellemare-Pelletier, A.; Laplante, A.; Rondeau, C.; Chemali, M.; Fazel, A.; Bergeron, J.J.; Trudeau, L.E.; Burelle, Y.; et al. Parkinson's Disease-Related Proteins PINK1 and Parkin Repress Mitochondrial Antigen Presentation. *Cell* **2016**, *166*, 314-327, doi:10.1016/j.cell.2016.05.039.
17. Veroni, C.; Aloisi, F. The CD8 T Cell-Epstein-Barr Virus-B Cell Trialogue: A Central Issue in Multiple Sclerosis Pathogenesis. *Front Immunol* **2021**, *12*, 665718, doi:10.3389/fimmu.2021.665718.
18. Mouat, I.C.; Shanina, I.; Horwitz, M.S. Age-associated B cells are long-lasting effectors that impede latent gammaHV68 reactivation. *Sci Rep* **2022**, *12*, 21189, doi:10.1038/s41598-022-25543-1.
19. Golinski, M.L.; Demeules, M.; Derambure, C.; Riou, G.; Maho-Vaillant, M.; Boyer, O.; Joly, P.; Calbo, S. CD11c(+) B Cells Are Mainly Memory Cells, Precursors of Antibody Secreting Cells in Healthy Donors. *Front Immunol* **2020**, *11*, 32, doi:10.3389/fimmu.2020.00032.
20. Mouat, I.C.; Allanach, J.R.; Fettig, N.M.; Fan, V.; Girard, A.M.; Shanina, I.; Osborne, L.C.; Vorobeychik, G.; Horwitz, M.S. Gammaherpesvirus infection drives age-associated B cells toward pathogenicity in EAE and MS. *Sci Adv* **2022**, *8*, eade6844, doi:10.1126/sciadv.ade6844.
21. Sachinidis, A.; Garyfallos, A. Involvement of age-associated B cells in EBV-triggered autoimmunity. *Immunol Res* **2022**, *70*, 546-549, doi:10.1007/s12026-022-09291-y.

22. Guo, Z.; Su, Y.; Lou, H. GFAP-Positive Progenitor Cell Production is Concentrated in Specific Encephalic Regions in Young Adult Mice. *Neurosci Bull* **2018**, *34*, 769-778, doi:10.1007/s12264-018-0228-4.
23. Arellano, J.I.; Duque, A.; Rakic, P. A coming-of-age story: adult neurogenesis or adolescent neurogenesis in rodents? *Front Neurosci* **2024**, *18*, 1383728, doi:10.3389/fnins.2024.1383728.
24. Tur, C.; Carbonell-Mirabent, P.; Cobo-Calvo, A.; Otero-Romero, S.; Arrambide, G.; Midaglia, L.; Castillo, J.; Vidal-Jordana, A.; Rodriguez-Acevedo, B.; Zabalza, A.; et al. Association of Early Progression Independent of Relapse Activity With Long-term Disability After a First Demyelinating Event in Multiple Sclerosis. *JAMA Neurol* **2023**, *80*, 151-160, doi:10.1001/jamaneurol.2022.4655.
25. Srivastava, S. The Mitochondrial Basis of Aging and Age-Related Disorders. *Genes (Basel)* **2017**, *8*, doi:10.3390/genes8120398.
26. Shen, Y.; Jiang, W.L.; Li, X.; Cao, A.L.; Li, D.; Li, S.Z.; Yang, J.; Qian, J. Mitochondrial dynamics in neurological diseases: a narrative review. *Ann Transl Med* **2023**, *11*, 264, doi:10.21037/atm-22-2401.
27. Etemadifar, M.; Afshar, F.; Nasr, Z.; Kheradmand, M. Parkinsonism associated with multiple sclerosis: A report of eight new cases and a review on the literature. *Iran J Neurol* **2014**, *13*, 88-93.
28. Sadnicka, A.; Sheerin, U.M.; Kaplan, C.; Molloy, S.; Muraro, P.A. Primary progressive multiple sclerosis developing in the context of young onset Parkinson's disease. *Mult Scler* **2013**, *19*, 123-125, doi:10.1177/1352458512445942.
29. Cossu, D.; Yokoyama, K.; Sechi, L.A.; Hattori, N. Potential of PINK1 and PARKIN Proteins as Biomarkers for Active Multiple Sclerosis: A Japanese Cohort Study. *Front Immunol* **2021**, *12*, 681386, doi:10.3389/fimmu.2021.681386.
30. Joodi Khanghah, O.; Nourazarian, A.; Khaki-Khatibi, F.; Nikanfar, M.; Laghousi, D.; Vatankhah, A.M.; Moharami, S. Evaluation of the Diagnostic and Predictive Value of Serum Levels of ANT1, ATG5, and Parkin in Multiple Sclerosis. *Clin Neurol Neurosurg* **2020**, *197*, 106197, doi:10.1016/j.clineuro.2020.106197.
31. Tiku, V.; Tan, M.W.; Dikic, I. Mitochondrial Functions in Infection and Immunity: (Trends in Cell Biology 30, 263-275, 2020). *Trends Cell Biol* **2020**, *30*, 748, doi:10.1016/j.tcb.2020.07.001.
32. Xie, L.; Shi, F.; Li, Y.; Li, W.; Yu, X.; Zhao, L.; Zhou, M.; Hu, J.; Luo, X.; Tang, M.; et al. Drp1-dependent remodeling of mitochondrial morphology triggered by EBV-LMP1 increases cisplatin resistance. *Signal Transduct Target Ther* **2020**, *5*, 56, doi:10.1038/s41392-020-0151-9.
33. Ivan, I.; Irincu, L.; Diaconu, S.; Falup-Pecurariu, C. Parkinsonism associated with viral infection. *Int Rev Neurobiol* **2022**, *165*, 1-16, doi:10.1016/bs.irn.2022.07.005.
34. Tiwari, D.; Mittal, N.; Jha, H.C. Unraveling the links between neurodegeneration and Epstein-Barr virus-mediated cell cycle dysregulation. *Curr Res Neurobiol* **2022**, *3*, 100046, doi:10.1016/j.crneur.2022.100046.
35. Alvarez-Sanchez, N.; Dunn, S.E. Potential biological contributers to the sex difference in multiple sclerosis progression. *Front Immunol* **2023**, *14*, 1175874, doi:10.3389/fimmu.2023.1175874.
36. Lazarevic, M.; Stanisavljevic, S.; Nikolovski, N.; Dimitrijevic, M.; Miljkovic, D. Complete Freund's adjuvant as a confounding factor in multiple sclerosis research. *Front Immunol* **2024**, *15*, 1353865, doi:10.3389/fimmu.2024.1353865.
37. Cossu, D.; Tomizawa, Y.; Momotani, E.; Yokoyama, K.; Hattori, N. Adjuvant Activity of Mycobacterium paratuberculosis in Enhancing the Immunogenicity of Autoantigens During Experimental Autoimmune Encephalomyelitis. *J Vis Exp* **2023**, doi:10.3791/65422.
38. Noda, S.; Sato, S.; Fukuda, T.; Tada, N.; Uchiyama, Y.; Tanaka, K.; Hattori, N. Loss of Parkin contributes to mitochondrial turnover and dopaminergic neuronal loss in aged mice. *Neurobiol Dis* **2020**, *136*, 104717, doi:10.1016/j.nbd.2019.104717.